Supporting Information

Lin et al. 10.1073/pnas.1106453108

SI Materials and Methods

Circular Dichroism. Utrophin constructs were prepared in PBS, at 20-μM concentration. Proteins were clarified by ultracentrifugation at 100,000 × *g* for 15 min at 4 °C prior to sample preparation. CD spectra were acquired using a JASCO J-815 spectrophotometer and a temperature-jacketed spectral cell with a path length of 0.1 cm. Spectra were taken from 200 to 260 nm at intervals of 1 nm, bandwidth of 1 nm, and a 1-s averaging time with temperature set at 25 °C. Data were analyzed assuming that the CD spectrum is a linear combination of the contributions from α-helix, β-sheet, and random coil.

$$\mathrm{E}(\lambda) = x_\alpha E_\alpha(\lambda) + x_\beta E_\beta(\lambda) + x_R R_R(\lambda). \quad \textbf{[S1]}$$

The unit of E is molar ellipticity ($\mathrm{deg}^*\ \mathrm{cm}^2\ \mathrm{dmol}^{-1}$) per residue. The percent α-helix of the sample is similar between native Utr261, unlabeled V136C/L222C and N-(1-oxyl-2,2,6,6-tetramethyl-4-piperidinyl)maleimide (MSL)-labeled V136C/L222C. This indicated that the presence of the mutation or the attachment of MSL did not significantly alter the secondary structure of the CH domains (Fig. S1).

Cosedimentation Assay. Binding affinities of utrophin constructs were determined by mixing 25 μM with a range of actin concentrations (0–70 μM), then centrifuging at 100,000 × *g* for 20 min at 4 °C. Concentrations of free utrophin (U_F) were determined using a Bradford assay using a BSA standard (Biorad). Regression analysis was done fitting the data to $X_b = A/(A + K_d)$, where A is concentration of free actin protomers, X_b is the fraction of actin protomers with bound utrophin, and K_d is the dissociation constant. The K_d values determined for native Utr261, unlabeled V136C/L222C, and MSL-labeled V136C/L222C (Fig. S2) were very similar and within the range of K_d previously reported for Utr261 (1–3). Thus, the presence of the mutation or the attachment of MSL did not affect the affinity of the CH domains to bind to actin.

1. Moores CA, Kendrick-Jones J (2000) Biochemical characterisation of the actin-binding properties of utrophin. *Cell Motil Cytoskeleton* 46:116–128.
2. Winder SJ, et al. (1995) Utrophin actin binding domain: Analysis of actin binding and cellular targeting. *J Cell Sci* 108:63–71.
3. Rybakova IN, Humston JL, Sonnemann KJ, Ervasti JM (2006) Dystrophin and utrophin bind actin through distinct modes of contact. *J Biol Chem* 281:9996–10001.

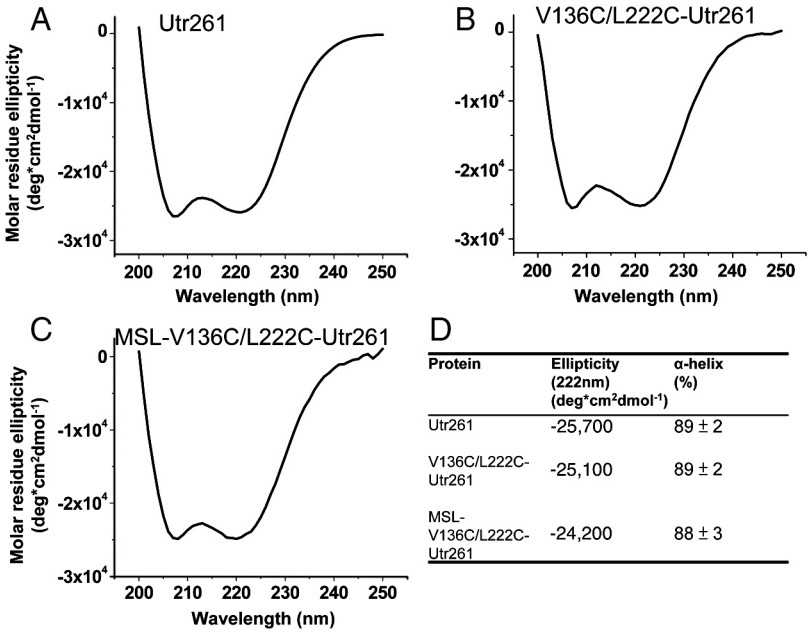

D

Protein	Ellipticity (222nm) (deg*cm²dmol⁻¹)	α-helix (%)
Utr261	-25,700	89 ± 2
V136C/L222C-Utr261	-25,100	89 ± 2
MSL-V136C/L222C-Utr261	-24,200	88 ± 3

Fig. S1. CD spectrum of (*A*) Utr261, (*B*) double mutant V136C/L222C, and (*C*) MSL-labeled V136C/L222C. (*D*) Percent α-helix determined from molar ellipticity at 222 nm with SD. Neither the presence of the double-cysteine mutations nor the MSL labeling disrupted the secondary structure.

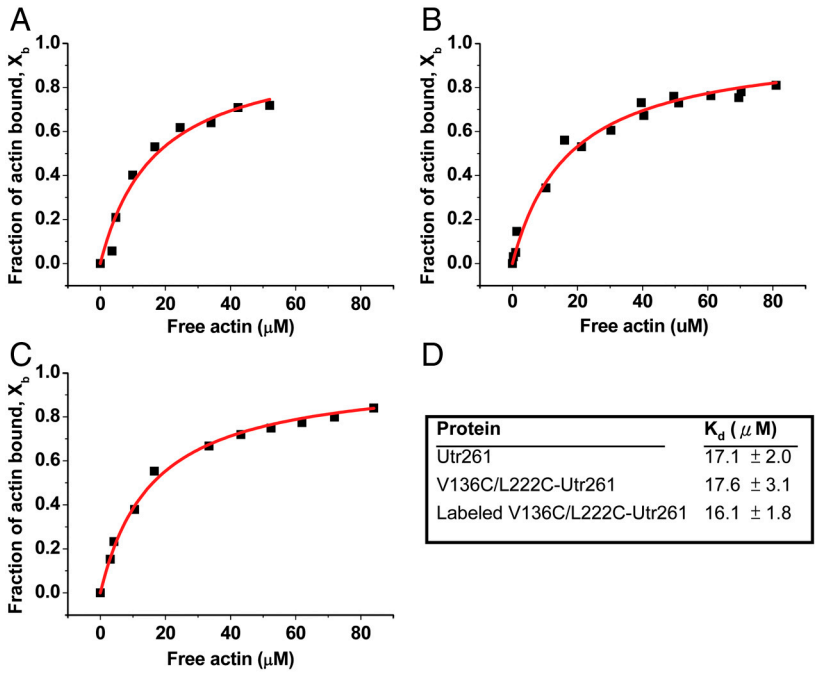

Protein	K_d (μM)
Utr261	17.1 ± 2.0
V136C/L222C-Utr261	17.6 ± 3.1
Labeled V136C/L222C-Utr261	16.1 ± 1.8

Fig. S2. Affinity of utrophin constructs binding to actin, defined by dissociation constant K_d, obtained from cosedimentation assays. Red curves show fits to $X_b = A/(A + K_d)$, where X_b is fraction of actin bound and A is free actin concentration. (*A*) Utr261, (*B*) unlabeled V136C/L222C-Utr261, and (*C*) MSL-labeled V136C/L222C-Utr261. (*D*) K_d values obtained from fits. Neither the double-cysteine mutations nor spin labeling affect the affinity of Utr261 for actin.

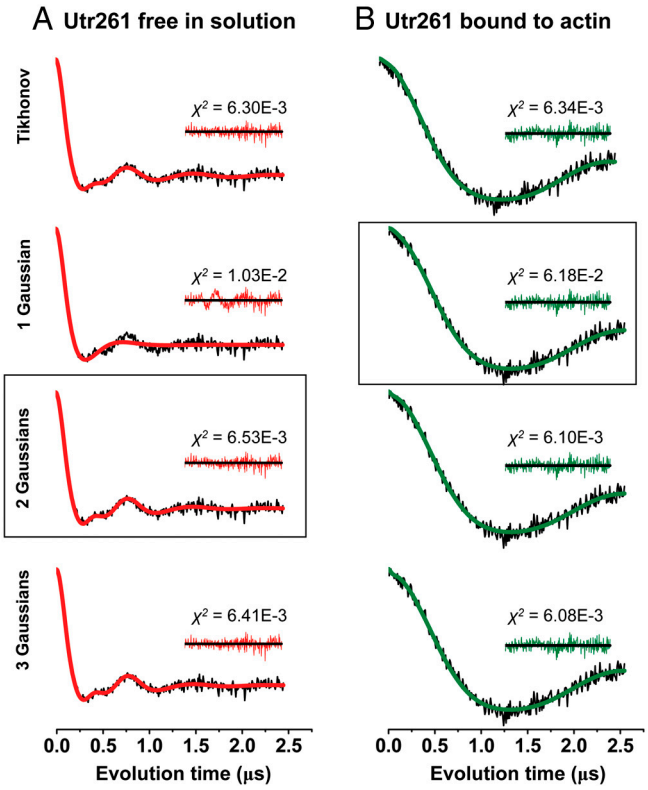

Fig. S3. Analysis of DEER data, by nonlinear least-squares fit, reveals two resolved conformational states. The top row shows the model-independent Tikhonov fit, while lower rows show the results of fits assuming models of Gaussian distance distributions. The number of Gaussian components was determined to be n (enclosed by boxes) when $n + 1$ did not significantly improve the residual or χ^2. (*A*) For Utr261 free in solution, a two-Gaussian fit ($n = 2$) is sufficient, because three Gaussians do not improve the fit. (*B*) When Utr261 is bound to actin, $n = 1$ is sufficient. Note that χ^2 values for the Tikhonov fits are virtually identical to those for the best Gaussian fits.

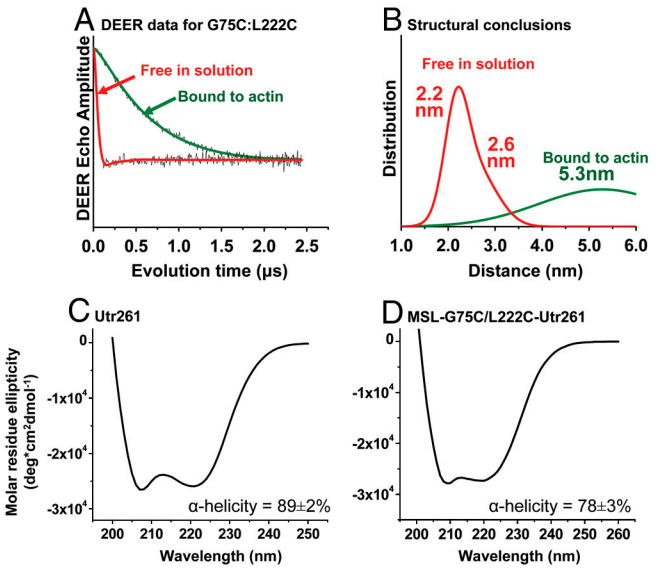

Fig. S4. (*A* and *B*) DEER data from the G75C/L222C mutant of Utr261, confirming the much slower oscillation (longer interdomain distance) observed in the actin-bound state (5.3-nm mean distance, green) compared with the free state (2.2-nm and 2.6-nm mean distances, red. The populations are 49% and 51%, respectively). The 5.3-nm distance was used as a second constraint in modeling the Utr261-actin complex shown in Fig. 5. (*C* and *D*) A significant disruption in secondary structure (detected by CD) is induced by mutation and labeling G75C/L222C, compared with mutation and labeling V136C/L222C (Fig. S1), which probably explains the broader distance distributions observed by DEER (compare Fig. S4*B* with Fig. 1*F*).

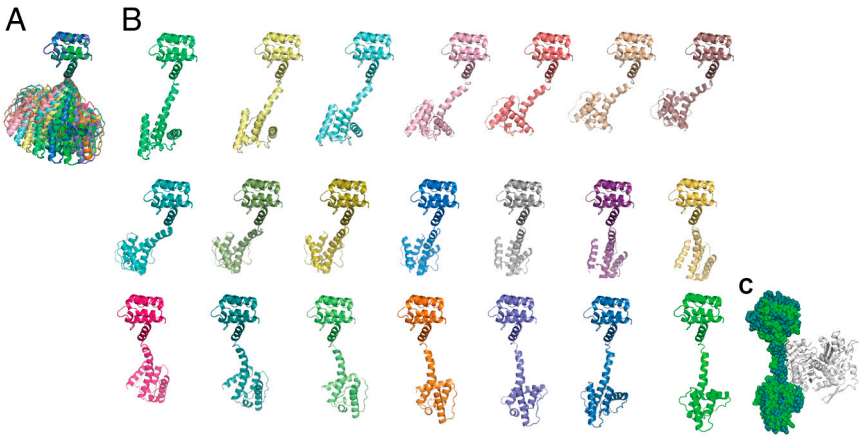

Fig. S5. Twenty-one simulated models of the actin-bound Utr246. (*A*) Compilation of all 21 models and (*B*) individual models. These models were simulated by rigid body rotations with a pivot point set at the peptide bond between residues 149 and 150 using distance measurements between labeling sites at C136 to C222 and C75 to C222 as constraints. A total of 21 models were generated. The one at the lower right corner (green) had the highest resemblance to the singly decorated "open 2" model (cyan), as is shown by the space filling model in *C*.